Redox Biology 50 (2022) 102237

Contents lists available at ScienceDirect

Redox Biology

journal homepage: www.elsevier.com/locate/redox

# NAMPT mitigates colitis severity by supporting redox-sensitive activation of phagocytosis in inflammatory macrophages

Sun Mi Hong [a], A-Yeon Lee [a,b], Sung-Min Hwang [a], Yu-Jin Ha [a,b], Moo-Jin Kim [a,b], Seongki Min [a,b], Won Hwang [c], Gyesoon Yoon [a,b], So Mee Kwon [d], Hyun Goo Woo [b,d], Hee-Hoon Kim [e], Won-Il Jeong [e], Han-Ming Shen [f], Sin-Hyeog Im [g,h], Dakeun Lee [i,*], You-Sun Kim [a,b,**]

[a] Department of Biochemistry, Ajou University School of Medicine, 164 Worldcup-ro, Yeongtong-gu, Suwon, Gyeonggi-do, 16499, Republic of Korea
[b] Department of Biomedical Sciences, Graduate School of Ajou University, 164 Worldcup-ro, Yeongtong-gu, Suwon, Gyeonggi-do, 16499, Republic of Korea
[c] MSBIOTECH. LTD, Chungbuk, 27672, Republic of Korea
[d] Department of Physiology, Ajou University School of Medicine, 164 Worldcup-ro, Yeongtong-gu, Suwon, Gyeonggi-do, 16499, Republic of Korea
[e] Laboratory of Liver Research, Graduate School of Medical Science and Engineering, Korea Advanced Institute of Science and Technology, Daejeon, Republic of Korea
[f] Faculty of Health Sciences, University of Macau, Macau, China
[g] Department of Life Sciences, Pohang University of Science and Technology, Pohang, 37673, Republic of Korea
[h] ImmunoBiome, Bio Open Innovation Center, Pohang, 37673, Republic of Korea
[i] Department of Pathology, Ajou University School of Medicine, 164 Worldcup-ro, Yeongtong-gu, Suwon, Gyeonggi-do, 16499, Republic of Korea

ARTICLE INFO

*Keywords:*
NAMPT
Colitis
Macrophage
Phagocytic activity
$NAD^+$
Inflammatory bowel disease

ABSTRACT

Nicotinamide phosphoribosyltransferase (NAMPT) is the rate-limiting enzyme in the nicotinamide adenine dinucleotide ($NAD^+$) salvage pathway and plays a crucial role in the maintenance of the $NAD^+$ pool during inflammation. Considering that macrophages are essential for tissue homeostasis and inflammation, we sought to examine the functional impact of NAMPT in inflammatory macrophages, particularly in the context of inflammatory bowel disease (IBD). In this study, we show that mice with NAMPT deletion within the myeloid compartment (*Nampt*$^{f/f}$*LysMCre*$^{+/-}$, *Nampt* mKO) have more pronounced colitis with lower survival rates, as well as numerous uncleared apoptotic corpses within the mucosal layer. *Nampt*-deficient macrophages exhibit reduced phagocytic activity due to insufficient $NAD^+$ abundance, which is required to produce NADPH for the oxidative burst. Nicotinamide mononucleotide (NMN) treatment rescues NADPH levels in *Nampt* mKO macrophages and sustains superoxide generation via NADPH oxidase. Consequently, *Nampt* mKO mice fail to clear dead cells during tissue repair, leading to substantially prolonged chronic colitis. Moreover, systemic administration of NMN, to supply $NAD^+$, effectively suppresses the disease severity of DSS-induced colitis. Collectively, our findings suggest that activation of the NAMPT-dependent $NAD^+$ biosynthetic pathway, via NMN administration, is a potential therapeutic strategy for managing inflammatory diseases.

; 6AN, 6-aminonicotinamide; BMDM, Bone marrow-derived macrophage; CD, Crohn's disease; DAI, Disease activity index; DEG, Differentially expressed gene; DPI, Diphenyleneiodonium chloride; DSS, Dextran sulfate sodium; EpCAM, Epithelial cell adhesion molecule; IBD, Inflammatory bowel disease; IFN, Interferon; IL, Interleukin; LPS, Lipopolysaccharide; mKO, Myeloid-specific knock out; NAD, Nicotinamide adenine dinucleotide; NAM, Nicotinamide; NAMPT, Nicotinamide phosphoribosyltransferase; NMN, Nicotinamide mononucleotide; NOX2, NADPH oxidase 2; PBMC, Peripheral blood mononuclear cell; ROS, Reactive oxygen species; SIRT, Sirtuin; TLR, Toll-like receptor; UC, Ulcerative colitis; WT, Wild type.

* Corresponding author. Department of Pathology, Ajou University School of Medicine164 Worldcup-ro, Yeongtong-gu, Suwon, Gyeonggi-do, 16499, Republic of Korea.

** Corresponding author. Department of Biochemistry, Ajou University School of Medicine, 164 Worldcup-ro, Yeongtong-gu, Suwon, Gyeonggi-do, 16499, Republic of Korea.

*E-mail addresses:* dakeun@ajou.ac.kr (D. Lee), yousunkim@ajou.ac.kr (Y.-S. Kim).

https://doi.org/10.1016/j.redox.2022.102237
Received 30 November 2021; Received in revised form 5 January 2022; Accepted 12 January 2022
Available online 15 January 2022

## 1. Introduction

Inflammation is characterized by a sequence of events comprising an activation phase, which is designed to allow rapid and robust immune responses that are required to eliminate invading pathogens [1,2]. The subsequent resolution phase is an active process controlled by the accumulation of activated macrophages with pro-resolving capacity for rapid return to homeostasis [3–5]. Intestinal macrophages play a key role in fine-tuning the mucosal immune system and in the innate immune response, wherein they contribute to the production of cytokines, growth factors, and lipid mediators [6,7]. Moreover, intestinal macrophages function to clear pathogens, bacterial wall components, and apoptotic cells [8]. Failure to mount a robust protective response against pathogens during the resolution phase of inflammation may lead to persistent and excessive inflammation, as often observed in the pathogenesis of inflammatory bowel diseases (IBD) [9,10]. Recently, genome-wide association studies have identified key driver genes in macrophages leading to IBD [11]. Additionally, accumulating evidence supports the notion that enforcing a pro-resolving phenotype in macrophages might represent a novel therapeutic approach for the control of intestinal inflammation and restoration of tissue function.

Nicotinamide phosphoribosyl-transferase (NAMPT) catalyzes the synthesis of nicotinamide mononucleotide (NMN) from nicotinamide (NAM) and 5′-phosphoribosyl-1′-pyrophosphate (PRPP), thus playing an important role in the cyclic biosynthetic pathway of nicotinamide adenine dinucleotide ($NAD^+$) [12,13]. $NAD^+$ is essential for the maintenance of cellular energy via redox reactions and acts as a substrate for $NAD^+$-cleaving enzymes, such as poly (ADP-ribose) polymerases, sirtuins (SIRTs), and cADP-ribose synthases (e.g. CD38/CD157) [14–16]. $NAD^+$ is produced by two distinct biosynthetic pathways, namely, the salvage and *de novo* pathways [17]. As the rate-limiting enzyme in the $NAD^+$ salvage pathway, NAMPT is biologically indispensable and implicated in various inflammatory diseases, including rheumatoid arthritis, diabetes, and sepsis [18–22]. However, the role of NAMPT in inflammatory macrophages has not been fully elucidated, particularly in the context of IBD.

Herein, we investigated the functions and underlying molecular mechanisms of NAMPT in a murine dextran sulfate sodium (DSS)-induced colitis model with *Nampt* deletion in the myeloid compartment (*Nampt*$^{f/f}$*LysMCre*$^{+/-}$, *Nampt mKO*). *Nampt* deletion in macrophages impaired their phagocytosis functions due to the defect in $NAD^+$ supply, leading to increased severity of colitis. Finally, administration of NMN improved the survival rate of *Nampt* mKO mice with DSS-induced colitis. We believe that our study provides insights for the development of a novel therapeutic strategy, via activating the NAMPT-dependent $NAD^+$ biosynthetic pathway, for inflammatory diseases, including IBD.

## 2. Material and methods

### 2.1. Transcriptome profiling in human peripheral blood mononuclear cells (PBMCs)

Affymetrix HG-U133A human GeneChip array data (NCBI GEO accession number: GSE3365) were used herein [23]. Differentially expressed genes (DEGs) in the PBMCs from patients with ulcerative colitis (UC; n = 26) and Crohn's disease (CD; n = 59), as well as normal healthy control individuals (NT, n = 42) were identified using the permutated Student's *t*-test. Gene ontology analysis was performed using the gProfileR in the R package. Additionally, using *xCell* [24], the properties of immune cells in each sample were investigated.

### 2.2. Nampt knockout mouse model

*Nampt*$^{f/f}$ mice (C57BL6) bearing two loxP sites flanking exon 5 were cross-bred with *LyzM-Cre* mice (C57BL6) to specifically knock out (KO) *Nampt* in the myeloid cell lineage, including macrophages (termed *Nampt*$^{f/f}$*LysMCre*$^{+/-}$, *Nampt mKO*). We used *Nampt*$^{f/f}$*LyzM-Cre*$^{+/-}$(heterozygous) as myeloid-specific *NAMPT*-depleted mice, and *Nampt*$^{f/f}$*LyzMCre*$^{-/-}$ (WT) as the control mice. Mice were housed in the Laboratory Animal Research Center of Ajou University and were maintained according to the guidelines of the Institutional Animal Care and Use Committee, who approved all animal procedures (2020–0013).

### 2.3. Mouse models of colitis

Age- and sex-matched *Nampt*$^{f/f}$ and *Nampt*$^{f/f}$*LyzMCre*$^{\pm}$ mice received 2.5% DSS (MP Biomedicals, Santa Ana, CA, USA) for 7 days, and were then allowed to recover for 7 days. NMN (500 mg/kg; Cayman, Ann Arbor, MI, USA) was administered via intraperitoneal injection three times per week from day 1 to termination of experiments. Colitis severity was determined daily via a scoring system based on the sum of the points for the following parameters: weight loss (0 points: no weight loss/weight gain, 1 point: 5–10% weight loss, 2 points: 11–15% weight loss, 3 points: 16–20% weight loss, and 4 points: > 21% weight loss); stool consistency (0 points: normal and well-formed, 2 points: very soft and unformed, and 4 points: watery stool); and bleeding stool score (0 points: normal color, 2 points: reddish color, and 4 points: bloody stool). Therefore, the disease activity index (DAI) ranged from 0 to 12 [25].

### 2.4. Isolation of colon lamina propria cells

Cell isolation was performed as described previously with slight modifications [26]. Briefly, extraintestinal fat tissues and blood vessels were carefully removed; the colons were then opened longitudinally and washed with cold phosphate-buffered saline (PBS). Colon pieces were digested in collagenase D and 0.1 mg/mL DNase I for 40 min. The obtained cell suspensions were then passed through 100 μm strainers layered onto a Percoll gradient and centrifuged.

### 2.5. Flow cytometric analysis

Cell suspensions were stained on ice for 20 min in the dark with various combinations of fluorochrome-conjugated antibodies, including anti-CD45 (30-F11), anti-CD11b (M1/70), anti-F4/80 (BM8), anti-Ly6G (1A8), anti-Ly6C (HK1.4), anti-MHC II (M5/114.15.2), anti-CD11c (N418), anti-CD206 (MMR), and anti-CD86 (GL-1) (all from BioLegend, San Diego, CA, USA). Samples were acquired on a FACS Canto II flow cytometer (BD, Franklin Lakes, NJ, USA). Data were analyzed using the FlowJo™ Software (BD).

### 2.6. Histopathology and immunohistochemistry

Histology was scored in a blinded manner using a semiquantitative scoring system based on the sum of the points of the following parameters [27]: presence of ulcers: 0 = none, 1 = punctate, 2 = minimal, 3 = moderate, 4 = widespread; presence of inflammation: 0 = none, 1 = minimal, 2 = mild, 3 = moderate, 4 = severe; extent of inflammation: 0 = none, 1 = mucosal, 2 = mucosal + submucosal, 3 = mucosal + submucosal + muscle penetration, 4 = full thickness involvement. Immunohistochemistry was performed using rabbit anti-NAMPT (Bethyl Laboratories, TX, USA), rabbit anti-Ki-67 (Abcam, Cambridge, UK), rabbit anti-cleaved caspase3 (Cell Signaling Technology), rat anti-CD326 (EpCAM)-APC (Invitrogen), and rat anti-F4/80 (Abcam) antibodies.

### 2.7. Staining for apoptotic and engulfed cells

Cell death was assessed by TUNEL assay using Apoptag plus in situ apoptosis fluorescein detection kit (Merck) according to the manufacturer's instructions. TUNEL-positive signals were normalized to the total nuclei signals for each field. Engulfed cells were stained using the Apoptag ISOL dual fluorescence apoptosis detection kit (Millipore)

according to the manufacturer's instructions. Subsequently, the samples were incubated overnight with rat anti-F4/80 antibody. The fluorescence of each image was obtained by confocal micros copy (A1R HD25, Nikon, Tokyo, Japan) and a slide scanner (Axioscan, Zeiss, Germany).

### 2.8. Phagocytosis evaluation

pHrodo™ Green-conjugated *Escherichia coli* Bioparticles™ were diluted in serum media and incubated for 30 min, followed by two washes with PBS. Cells were incubated for the indicated times and analyzed using a FACS Canto II flow cytometer (BD) or a fluorescence microscope (DFC3000G; Leica, Wetzlar, Germany).

### 2.9. Measurement of $NAD^+$, NADPH, and ATP

Bone marrow-derived macrophages (BMDMs) were harvested and analyzed using the EnzyChrom $NAD^+$/NADH Assay Kit (Bioassay Systems, Hayward, CA, USA), Elite NADPH Assay Kit (eEnzyme, Gaithersburg, MD, USA), and CellTiter-Glo(R) Luminescent Cell Viability assay (Promega, Madison, WI, USA) according to the manufacturers' instructions.

### 2.10. Measurement of reactive oxygen species (ROS)

BMDMs or peritoneal macrophages were incubated with Hanks' balanced salt solution (HBSS) containing 5 μM CM-H2DCFDA (Invitrogen, Carlsbad, CA, USA) at 37 °C for 15 min. To measure mitochondrial ROS levels, cells were incubated with 5 μM MitoSOX (Invitrogen) for 15 min. Fluorescence levels were monitored using the FACS Canto II (BD).

### 2.11. Measurement of mitochondrial membrane potential

BMDMs were incubated with HBSS containing 100 nM MitoTracker™ Green FM (Invitrogen) plus 400 nM MitoTracker™ Red CMXRos (Invitrogen) for 15 min at room temperature. Fluorescence levels were monitored using the FACS Canto II (BD).

### 2.12. Statistical analysis

Data were analyzed using the unpaired two-tailed Student's *t*-test with GraphPad Prism 9 (San Diego, CA) and are presented as the mean ± standard error of the mean (SEM). Statistical significance was set at $p < 0.05$.

## 3. Results

### 3.1. NAMPT expression is increased within the inflammation niche

We first analyzed NAMPT expression in various human tissue samples (data retrieved from BioGPS website, GSE1133) and found that whole blood cells had the highest *NAMPT* expression levels (Fig. 1a). We further analyzed NAMPT expression in a subtype of immune cells and observed that myeloid cells exhibited relatively higher levels of NAMPT in both humans and mice (Supplementary Fig. 1a). To better understand the relevance of NAMPT expression in inflammatory disorders, we analyzed transcriptome data (GSE3365) [23] for PBMCs from patients with ulcerative colitis (UC) and Crohn disease (CD), as well as normal

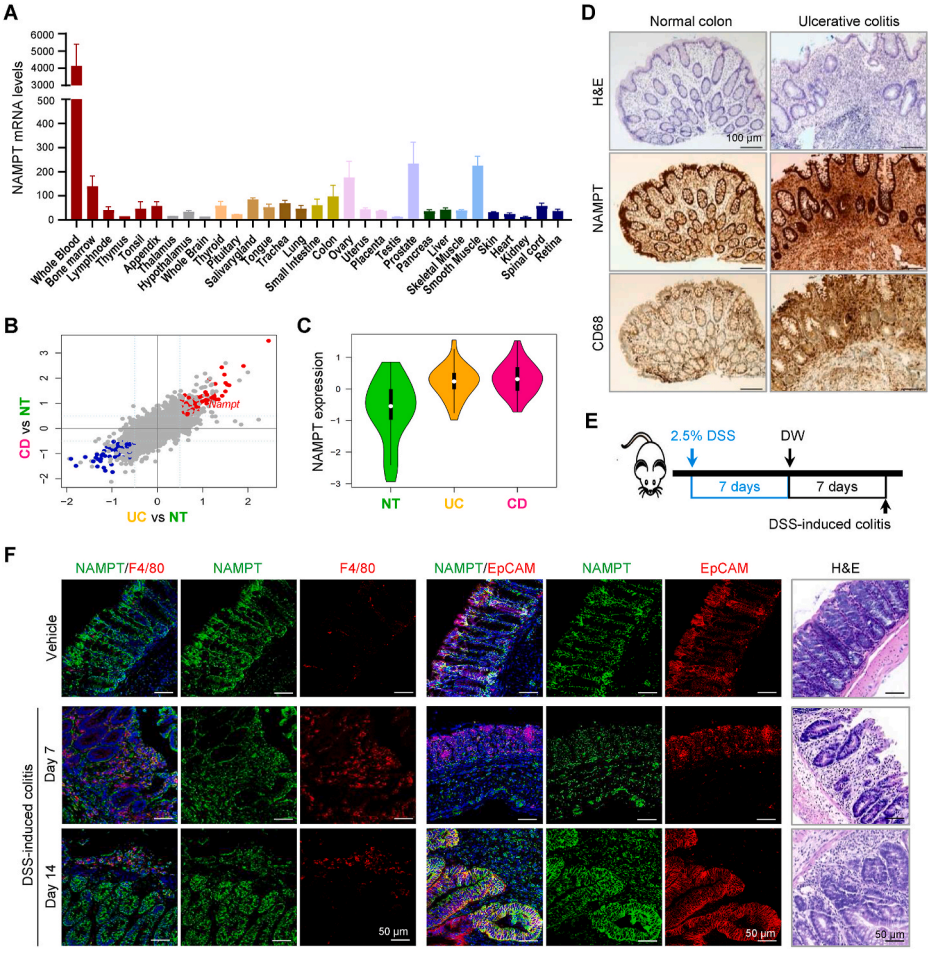


**Fig. 1.** Altered NAMPT expression pattern in inflammatory tissues and cells.
(A) Human *NAMPT* mRNA levels in various tissues for data retrieved from the BioGPS website. (B) Scattered dot plots showing the log2 fold difference between UC and NC or between CD and NC samples. Significantly up-or down-regulated genes are marked in red or dark blue color, respectively. (C) Violin plot showing *NAMPT* expression in PBMCs from NC, UC, or CD. (D) Immunohistochemistry for CD68 and NAMPT in normal and inflamed colon mucosae from UC patients. (E) DSS-induced colitis model. Mice were treated with 2.5% DSS for 7 days and were evaluated at day 14. (F) Paraffin-embedded colonic sections from DSS-treated mice were stained with hematoxylin and eosin and anti-NAMPT, anti-F4/80, and anti-EpCAM antibodies. . (For interpretation of the references to color in this figure legend, the reader is referred to the Web version of this article.)

control (NC). We identified commonly up-regulated (n = 107) and down-regulated (n = 126) genes in both UC and CD patients compared to NC (Supplementary Fig. 1b). Moreover, gene ontology analysis indicated that these up-regulated genes were highly related to leukocyte-mediated immunity, suggesting their pathological roles in inflammation (Supplementary Fig. 1c). As expected, *NAMPT* was among the up-regulated genes (Fig. 1b and c). Furthermore, immune profiling based on the transcriptome data revealed that myeloid cells were increased in the PBMCs from IBD patients (Supplementary Fig. 1d), suggesting that up-regulated expression of NAMPT in PBMCs from IBD patients may reflect an increased population of myeloid cells that play an important role in the process of inflammation. Since NAMPT expression in colon biopsies has been suggested as a marker of the severity of pediatric IBD [28], we next analyzed NAMPT expression in colon biopsies from IBD patients. Colon biopsies from UC patients showed higher numbers of inflammatory cells including CD68-positive macrophages, increased tissue fibrosis, and stronger NAMPT expression in inflamed areas, than did normal colon tissues (Fig. 1d).

To further establish the pathophysiological role of up-regulated NAMPT in inflammatory diseases, we used a DSS-induced colitis mouse model (Fig. 1e) and found destruction of the colonic epithelial structure, increased span of inflamed areas, thicker mucosa, and substantial F4/80$^{+}$ macrophage population on day 7, whereas these were largely recovered by day 14 (Fig. 1f). Under normal condition, NAMPT is primarily expressed in the epithelium and colocalized with epithelial cell adhesion molecule (EpCAM), as shown in Fig. 1f. However, in DSS-induced colitis, NAMPT expression was detected in epithelium as well as in lamina propria, wherein NAMPT was colocalized with F4/80 on day 7. These data indicate that up-regulated NAMPT expression in inflamed tissues is not only transcriptionally regulated, but also results from increased recruitment of macrophages to the inflammatory sites.

### 3.2. NAMPT deficiency in macrophages augments colitis severity

To investigate the role of myeloid-specific NAMPT in inflammation, we generated mice with specific *Nampt* deletion in the myeloid compartment (*Nampt$^{f/f}$LysMCre$^{+/-}$*) (Fig. 2a, upper panel). NAMPT protein expression in different tissues from both *Nampt$^{f/f}$* (wild type, WT) and *Nampt$^{f/f}$LysMCre$^{+/-}$* (mKO) mice showed a similar pattern (Supplementary Fig. 2a). Importantly, compared to those in WT mice, NAMPT protein levels in total bone marrow-derived monocytes (BMs) from *Nampt* mKO mice decreased by 38% (Supplementary Fig. 2b) but were undetectable in the peritoneal macrophages of *Nampt* mKO mice, which indicates successful macrophage-specific deletion of *Nampt* (Fig. 2a, lower panel and Supplementary Fig. 2c). Of note, the proportion of F4/80$^{+}$ cells within BMDMs (Mφ) were similar between WT and *Nampt* mKO mice (Fig. 2b).

Using this mouse model, we investigated the role of NAMPT in inflammatory macrophages in DSS-induced colitis. After colitis induction, WT mice typically lost 10% of their body weight by day 10, however, all regained their weight and survived (Fig. 2c and d). In contrast, *Nampt* mKO mice showed body weight loss by 24% and 42% of *Nampt* mKO mice died of disease (Fig. 2c and d). Additionally, a marked difference was observed in the DAI score between WT and *Nampt* mKO mice, suggesting a protective role of macrophage-derived NAMPT in the context of colitis (Fig. 2e). In fact, 14 days after DSS treatment, the colon length became significantly shorter in *Nampt* mKO than in WT mice (Fig. 2f). Moreover, observer-blinded pathological analyses revealed a

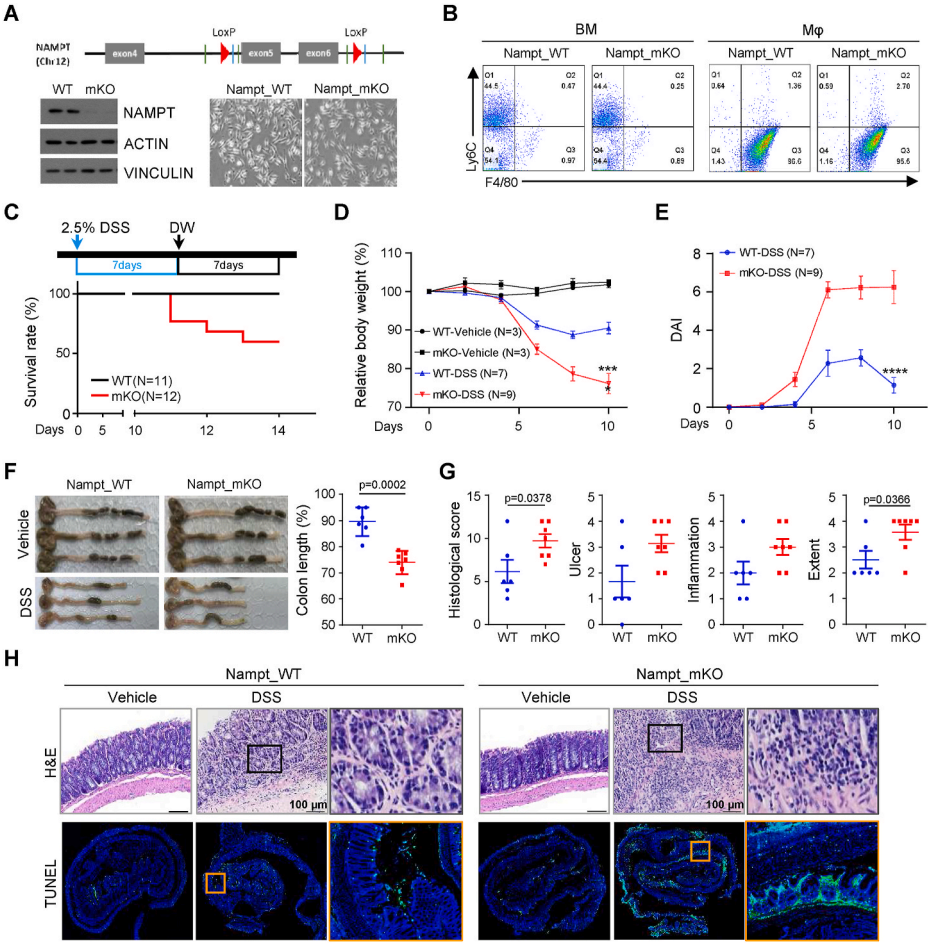


**Fig. 2.** Loss of NAMPT in macrophages enhances DSS-induced colitis.
(A) Macrophage-specific *Nampt* knockout mice obtained via the crossing of *Nampt$^{f/f}$* mice with lysozyme M-Cre driver mice. Representation of the *Nampt* locus inserted with the flox sequences flanking in front of exon 5 and behind exon 6 (upper panel). NAMPT protein levels in BMDMs from 2-month-old *Nampt$^{f/f}$* (wild type; WT) and *Nampt$^{f/f}$LyzMCre$^{+/-}$* (knockout; *Nampt* mKO) mice (left panel). Cell morphology of BMDMs from WT and *Nampt* mKO mice (right panel). (B) Bone marrow (BM) cells were isolated from WT and *Nampt* mKO mice and were differentiated into macrophages with M-CSF. The expression of Ly6C and F4/80 was evaluated by flow cytometry. (C, D) Survival curve (C) and relative body weight of 2.5%-DSS-treated mice (D). (E) Disease activity index (DAI) was scored based on stool consistency, fecal bleeding, and weight loss. The individual parameters were scaled from 0 to 4 (0–12 in total) as described in the materials and methods section. (F) Representative images of DSS-induced colitis. The colon lengths of DSS-induced mice were measured. (G) The histological score of the colon was calculated based on hematoxylin and eosin (H&E)-stained colon sections. (H) Representative images of H&E and TUNEL staining of colon tissues. Scale bar = 100 μm. Results are represented as the mean ± SEM. Statistical analysis was performed using the unpaired 2-tailed Student's *t*-test.

significantly greater histological score and a prominent tissue destruction, as well as severe inflammation and ulceration in DSS-treated *Nampt* mKO mice than in WT mice (Fig. 2g and h). Furthermore, *Nampt* mKO mice had more TUNEL $^{+}$ cells in colonic tissues than WT mice (Fig. 2h). Collectively, these results suggest that macrophage-specific *Nampt* deletion increases the severity of DSS-induced colitis in this mouse model.

### 3.3. *Nampt* deletion does not affect initial inflammatory response in DSS-induced colitis

For a successful resolution of inflammation, macrophages act in a sequential and coordinated cascade; clearing a pathogen, terminating inflammatory response, and repairing damaged tissue [29]. To better delineate the contribution of NAMPT in DSS-induced colitis, we compared disease activities on the first day 7 (induction period) and the subsequent 7 days (recovery period) (Fig. 3a left panel). Although *Nampt* mKO mice showed severe body weight loss and shortening of the colon on day 14, the difference between WT and *Nampt* mKO mice in colon length was not statistically significant on day 7 (Fig. 3a right panel and Supplementary Fig. 3a). Marked inflammation and tissue destruction along with many macrophages infiltration were also noted on day 7 in the colon of both WT and *Nampt* mKO mice (Fig. 3b). However, unlike the *Nampt* mKO mice, the WT mice seemed to recover from the injury, as evidenced by the restored colon length (see Fig. 2f) and reduced number of infiltrated macrophages on day 14 (Fig. 3b).

We next measured the proportions of monocytes and macrophages on day 7 and found similar proportions between WT and *Nampt* mKO mice (Fig. 3c and Supplementary Figs. 3b and c). Of note, the proportions of pro-inflammatory Ly6C$^{high}$MHC-II$^{low}$ macrophages and Ly6C$^{low}$ MHC-II$^{high}$ macrophages were also similar between *Nampt* mKO and WT mice (Fig. 3d and Supplementary Fig. 3d), suggesting that

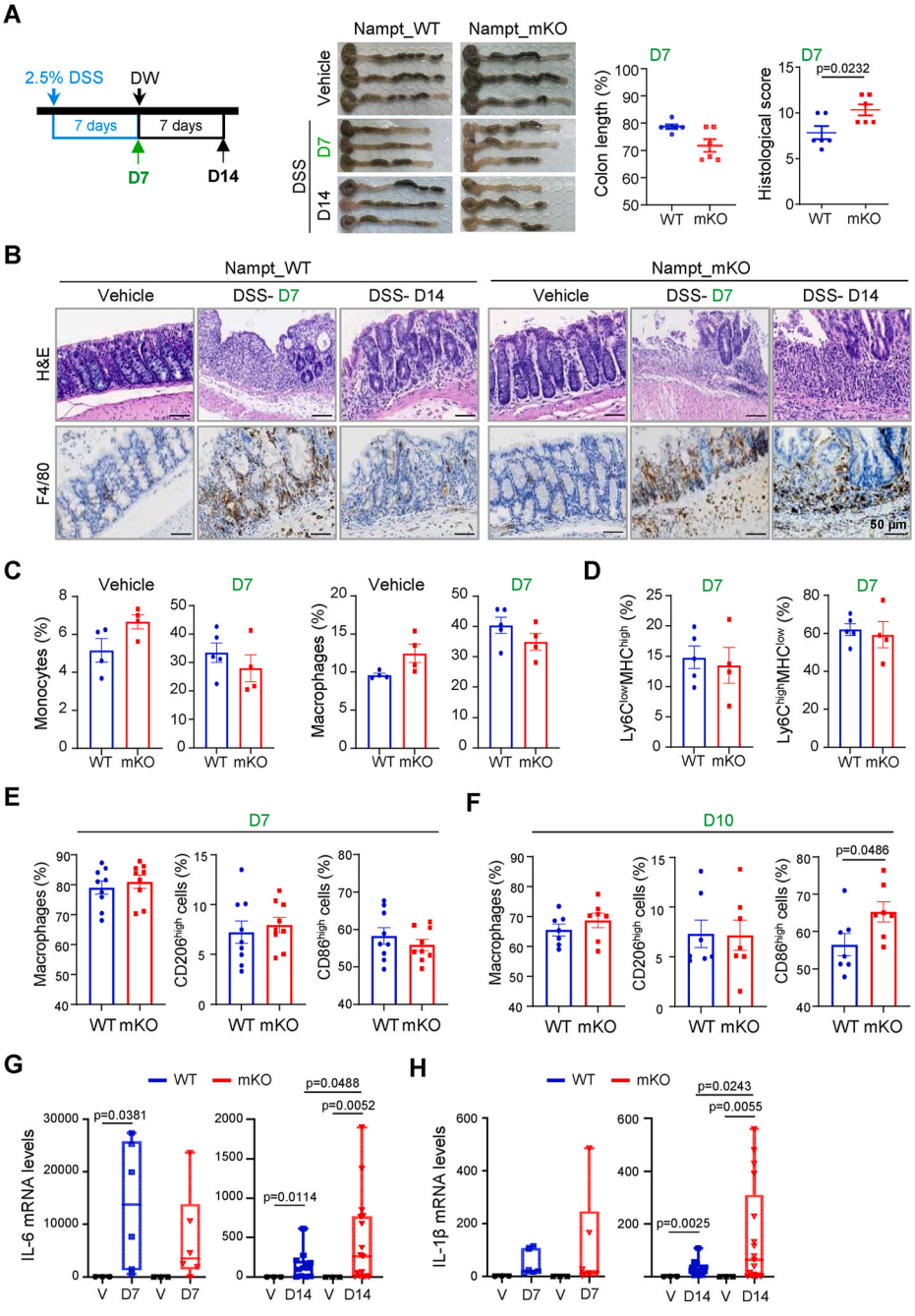


**Fig. 3.** *Nampt*-deleted macrophages did not alter initiation of inflammatory response.
(A) Mice were treated with 2.5% DSS for 7 days and evaluated at day 7 or 14. Representative image of the colons from DSS-treated mice. The histological scores were calculated based on hematoxylin and eosin (H&E)-stained colon sections obtained 7 days after DSS treatment. (B) Paraffin-embedded colonic sections from DSS-treated mice on days 7 and 14 were stained with H&E (upper) and anti-F4/80 antibody (down). Scale bar = 50 μm. (C, D) Lamina propria immune cells were isolated from the colons of DSS-treated mice at day 7. The percentages of monocytes (CD11b$^{+}$Ly6C$^{+}$), macrophages (CD11b$^{+}$F4/80$^{+}$), Ly6C$^{low}$MHCII$^{high}$, and Ly6C$^{high}$MHCII$^{low}$ macrophages were determined by flow cytometry. (E, F) Lamina propria immune cells were isolated from the colons of DSS-treated mice at day 7 and 10. The percentages of M1 macrophages (CD11b$^{+}$F4/80$^{+}$CD86$^{high}$) and M2 macrophages (CD11b$^{+}$F4/80$^{+}$CD206$^{high}$) were determined by flow cytometry. (G, H) Relative mRNA levels of cytokines in the colonic tissues of DSS-treated WT and *Nampt* mKO mice on day 7 and 14. The results are represented as the mean ± SEM. Statistical analysis was performed using the Student's *t*-test.

*Nampt* deletion in macrophages does not affect local recruitment of monocytes/macrophages and initial inflammatory response.

### 3.4. Colitis severity in Nampt mKO mice is not related to M1/M2 macrophage polarization

It has been reported that disequilibrium of M1 and M2 macrophage subsets promote colitis development and NAMPT contribute to the polarization and activation of M1 macrophages [28,30]. Therefore, we sought to determine whether deletion of *Nampt* alters colonic M1 and M2 macrophage populations during colitis. First, we analyzed the proportions of M1 and M2 macrophages in the colonic mucosa of DSS-induced colitis model. On day 7, the proportions of $F4/80^{+}CD11b^{+}$ macrophages, as well as M1 ($CD86^{high}$) and M2 ($CD206^{high}$) macrophages were similar between the *Nampt* mKO and WT mice upon DSS treatment (Fig. 3e). However, *Nampt* mKO mice had a higher population of M1 ($CD86^{high}$) macrophages than WT mice on day 10 (Fig. 3f).

M1 and M2 macrophages are characterized by the secretion of pro- and anti-inflammatory cytokines, respectively [31]. Similar to our observations regarding colonic M1 and M2 macrophage populations, although we observed a robust induction of inflammatory genes during DSS treatment on day 7, no statistically significant effects were induced by *Nampt* deletion (Fig. 3g and h). Meanwhile, following the recovery phase, *Nampt* mKO mice maintained a larger macrophage population (see Fig. 3b) within the inflamed tissues, resulting in up-regulated expression of inflammatory genes in intestinal samples, compared with WT mice (Fig. 3g and h). Next, we investigated whether NAMPT is involved in M1/M2 polarization. BMDMs (M0) could differentiate into M1-like macrophages (M1) upon stimulation with lipopolysaccharide (LPS)/interferon (IFN)-γ or M2-like macrophages (M2) upon treatment with interleukin (IL)-4 [31]. Deletion of *Nampt* did not alter M1/M2 polarization (Supplementary Fig. 4a) nor did inhibition of NAMPT enzymatic activity via FK866 treatment (Supplementary Fig. 4b). The expression level of specific markers representing different macrophage phenotypes was further analyzed by western blot. No significant differences were observed between WT and *Nampt* mKO macrophages (Supplementary Fig. 4c); indicating that NAMPT is not involved in M1/M2 macrophage polarization during the inflammatory process. Similar to FACS analysis, FK866 treatment had no effect on the expression of M1/M2 macrophage-specific markers (Supplementary Fig. 4d).

Reduced responsiveness to Toll-like receptor (TLR) activation has been suggested to represent impaired macrophage function [32]. BMDMs from the WT and *Nampt* mKO mice had no alteration in TLR4 downstream signaling, such as mitogen-activated protein kinase (MAPK) and nuclear factor (NF)-κB activation in response to LPS (Supplementary Fig. 5a). Moreover, In agreement with a previous report [33], NAMPT depletion decreased mRNA levels of certain cytokines upon LPS treatment (Supplementary Figs. 5b and c). However, the level of IL-1β was similar in WT and *Nampt* mKO BMDMs upon LPS treatment for 5 h (Supplementary Fig. 5d). Furthermore, inflammasome activation, which is the innate immune component responsible for activation of inflammatory responses, was also comparable between WT and *Nampt* mKO BMDMs (Supplementary Fig. 5e). Taken together, our data suggest that *Nampt* deletion in macrophages influences the severity of DSS-induced colitis, probably by inducing improper resolution of inflammation, whereas NAMPT depletion does not impair macrophage polarization or cytokine production.

### 3.5. NAMPT deficiency impairs apoptotic cell clearance in DSS-induced intestinal injury

Several key events are required for the successful resolution of inflammation, and effective removal of dying cells by macrophages is the essential for this [34]. Thus, as an indicator of tissue injury recovery, we measured $Ki67^{+}$ cells in DSS-induced colitis samples from WT and *Nampt* mKO mice on day 7. As expected, the percentage of Ki67+ cells in the epithelium, was markedly reduced in *Nampt* mKO mice (Fig. 4a). Additionally, to examine the role of NAMPT in apoptotic cell clearance *in vivo*, DSS-induced colitis samples from WT and *Nampt* mKO mice were stained with cleaved caspase-3 antibody to quantify the number of remaining uncleared apoptotic corpses. We found that significantly more positive signals were observed in *Nampt* mKO mice on day 14 (Fig. 4b). Similarly, the number of TUNEL+ nuclei in the epithelium of colon mucosa of *Nampt* mKO mice was significantly increased, compared to that of WT mice (Fig. 4c).

Next, we investigated whether NAMPT-deficient macrophages show decreased engulfment in the DSS-induced colitis model. To this end, we employed a detection method that can distinguish engulfed cells within phagocytes [35]. As the DNA derived from the engulfed debris undergoes DNase II-mediated cleavage (type II break) within a phagolysosome, we detected engulfed cells by monitoring type II DNA cleavage. As shown in Fig. 4d, signals of engulfed cells were higher in WT mice than in *Nampt* mKO mice. Furthermore, $F4/80^{+}$ macrophages exhibited a lower level of engulfed cells in colonic tissues from *Nampt* mKO mice. Collectively, these findings suggest that depletion of NAMPT in activated inflammatory macrophages could attenuate cell clearing activity, and in turn, augment colitis severity in this murine model.

### 3.6. Nampt-deleted macrophages exhibit attenuated phagocytic potential

In our *in vivo* DSS-induced colitis mouse model, we found that NAMPT functions in the phagocytosis of apoptotic cells during the inflammatory response. To further support this notion, we compared the phagocytic activity between the WT and *Nampt* mKO macrophages by performing a pulse and chase phagocytosis assay using pHrodo green. In WT BMDMs, an increase in the intensity of green fluorescence signals was observed, indicating the gradual maturation and fusion of pHrodo green containing phagosomes with lysosomes (Supplementary Fig. 6a). Although there was no difference in BMDM polarization upon LPS/IFN-γ treatment (see Supplementary Fig. 4a), green fluorescence intensity was markedly reduced in *Nampt* mKO BMDMs relative to that in WT BMDMs upon pHrodo challenge for 30 min (Fig. 5a). pHrodo intensity upon FK866 treatment in WT BMDMs was reduced, while treatment of NMN in *Nampt* mKO BMDMs rescued the fluorescence intensity (Fig. 5b and Supplementary Figs. 6b and c). Inhibition of NAMPT activity by FK866 also reduced pHrodo intensity in RAW264.7 cells, as shown in WT BMDMs (Fig. 5c). As expected, lysosome inhibitor, bafilomycin A1 (Baf A1) treatment reduced the fluorescence intensity of pHrodo in both WT BMDMs and RAW264.7 cells, indicating that the engulfed pHrodo green *E. coli* bioparticles containing phagosomes matured into late phagosomes or phagolysosomes, then the bioparticles were degraded in macrophages (Fig. 5d and Supplementary Fig. 6d). These results suggest that the enzymatic activity of NAMPT promotes macrophage phagocytosis.

ROS are essential bactericidal agents; NADPH oxidase 2 (NOX2) serves as the primary source of ROS in phagocytic immune cells [36]. Considering that our data suggests that NAMPT-depleted macrophages have impaired phagocytic activity, we next measured ROS levels upon LPS treatment in BMDMs from *Nampt* mKO and WT mice. *Nampt*-deleted BMDMs and peritoneal macrophages exhibited a defect in cellular ROS production upon LPS treatment (Fig. 5e and f). Of note, unlike the total cellular ROS levels, mitochondrial ROS levels and mitochondrial membrane potentials, upon LPS treatment, did not change significantly between WT and *Nampt* mKO macrophages (Fig. 5g and h). Additionally, in Raw 264.7 cells, treatment with FK866 partially inhibited ROS production in response to LPS, however, this inhibitory effect was reversed by $NAD^{+}$ co-treatment (Fig. 5i).

Furthermore, we examined whether inhibition of NOX2-mediated ROS generation can affect phagocytic activity. Using the NADPH oxidase inhibitor, diphenyleneiodonium chloride (DPI), we measured phagocytic activity in primary macrophages from WT and *Nampt* mKO

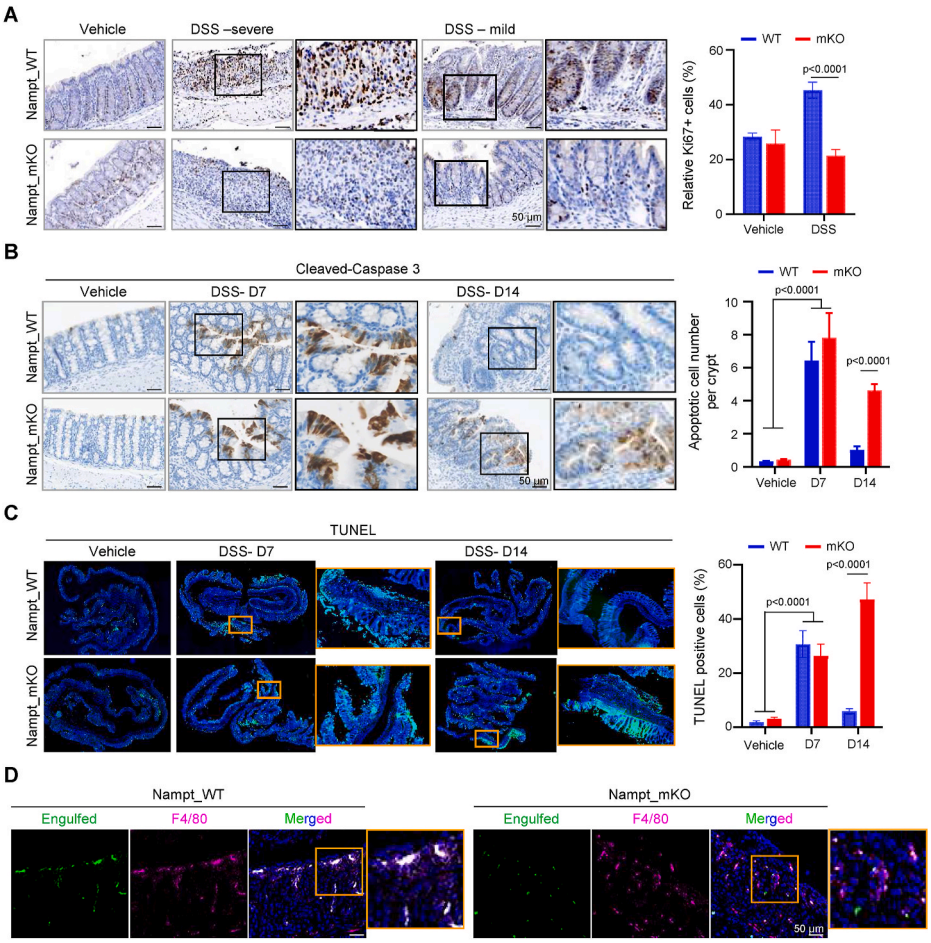


**Fig. 4.** Apoptotic cell clearance was attenuated in *Nampt*-deleted macrophages.
(A) Immunohistochemistry for Ki67 in the colonic tissues from mice treated with DSS for 7 days. Bar graphs represent percentage of positive cells out of total nuclei. (B) Immunohistochemistry for cleaved caspase-3 in the colonic tissues from mice treated with DSS at days 7 and 14. Bar graphs represent the number of positive cells per crypt. (C)
Sections of colon at days 7 and 14 were subjected to TUNEL staining. Representative images (left) and percentage of TUNEL-positive cells (right) are presented. (D) Staining of engulfed corpses and F4/80$^+$ macrophages in the colonic tissues from mice treated with DSS for 7 days. The results are represented as the mean ± SEM. Statistical analysis was performed using the unpaired 2-tailed Student's *t*-test. Scale bar = 50 μm.

mice. As expected, inhibition of NOX2 activity by DPI blocked phagocytic activity, indicating reduced NOX2-mediated ROS generation (Supplementary Fig. 6e). These results support that NAMPT expression in macrophages promotes phagocytosis in an enzymatic activity-dependent manner.

### 3.7. *NAMPT-deficient macrophages fail to produce sufficient NAD$^+$ for phagocytic activity*

Macrophages require NADPH as an electron carrier for ROS production [36]. Therefore, we hypothesized that NAMPT-deficient macrophages would show a defective phagocytic activity due to reduced NADPH levels (Fig. 6). As expected, NAMPT deficiency or FK866 treatment significantly reduced NAD$^+$ levels, while NMN administration rescued this phenotype (Fig. 6b and Supplementary Fig. 7a). As NAD$^+$ is a critical co-factor in ATP production, we next quantified ATP levels upon LPS treatment. No difference was observed in ATP levels under vehicle treatment between *Nampt* mKO and WT BMDMs, whereas LPS treatment decreased ATP levels in both cells (Fig. 6c), indicating that the process of ATP production is not directly mediated by NAMPT during the immune response.

Notably, NADPH levels were downregulated in *Nampt* mKO macrophages, while NMN administration increased NADPH levels (Fig. 6d), indicating that enzymatic activity of NAMPT regulates NADPH levels in BMDMs. LPS treatment markedly decreased NAD$^+$ levels, and FK866 treatment even caused a further reduction (Fig. 6e). Consistently, LPS challenge significantly reduced NADPH levels by 50% in WT macrophages. However, NADPH levels in NAMPT-depleted macrophages were reduced by 21% (Fig. 6f). Moreover, FK866 treatment caused a further decrease in NADPH levels, whereas NMN treatment restored NADPH levels under LPS treatment (Fig. 6g). These results suggest that NAMPT-depleted macrophages are unable to produce sufficient NADPH.

NAMPT promotes NADPH production via increasing NAD$^+$ influx into the pentose phosphate pathway (PPP) [37]. Of note, the oxidative burst requires a large amount of NADPH to fuel superoxide generation via NOX2 (Supplementary Fig. 7b). Consistently, we observed that treatment with 6-aminonicotinamide (6AN), an antimetabolite used to inhibit the PPP, reduced NADPH levels in a dose-dependent manner in WT, but not *Nampt* mKO macrophages (Fig. 6h). Furthermore, NMN administration rescued NADPH levels in *Nampt* mKO macrophages, which had been blocked by 6AN treatment (Fig. 6i). Under LPS challenge, inhibition of the PPP by 6AN further decreased NADPH levels (Fig. 6j). Expectedly, 6AN treatment led to a decrease in ROS level in BMDMs, which were stimulated with LPS and IFN-γ (Supplementary Fig. 7c). Taken together, our data suggest that NAMPT promotes NADPH production via the PPP to fuel NOX2 in the context of phagocytosis.

### 3.8. *NMN administration protects Nampt mKO mice from severe colitis*

We hypothesized that NAMPT deficiency in inflammatory macrophages does not provide sufficient NAD$^+$ in response to inflammation, leading to severe colitis via decreased NADPH levels. It is, therefore, assumed that the impact of NAMPT depletion on colitis might be alleviated by NMN supplementation. To test this hypothesis, we first examined the effect of NMN administration in a DSS-induced colitis model. After 2.5% DSS treatment, 500 mg/kg of NMN or PBS was injected intraperitoneally into *Nampt* mKO mice three times per week. NMN treatment alleviated body weight reduction and decreased DAI, resulting in a better survival rate (Fig. 7a and b; Supplementary Fig. 8a). In detail, PBS injection resulted in 33% survival (4/12 mice), whereas

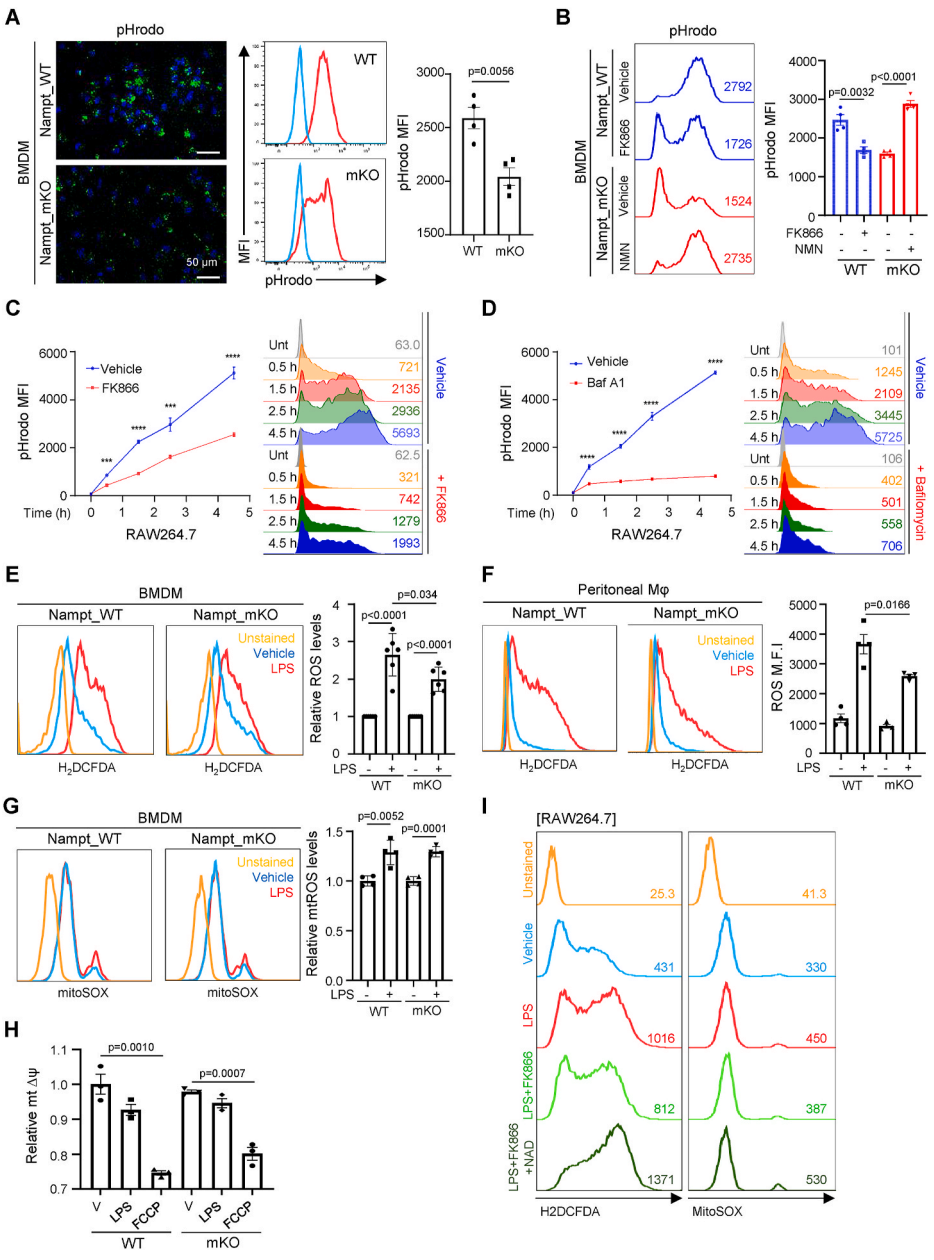


**Fig. 5.** NAMPT expression in macrophages is essential for optimal phagocytic activity.
(A) BMDMs from WT and *Nampt* mKO mice were treated with LPS/IFN-γ for 12 h. The phagocytic activity of BMDMs was detected at 30 min and 90 min after the addition of pHrodo green dye via fluorescence microscopy (Scale bar = 50 μm) (left), and the phagocytic activity of BMDMs was detected at 30 min after the addition of pHrodo green dye via flow cytometry (right). (B) The phagocytic activity of BMDMs was assessed in the presence of FK866 or NMN via flow cytometry. (C, D) The phagocytic activity of Raw 264.7 cells treated with 20 nM FK866 (C) and 50 nM Baf A1 (D) was assessed from 30 min to 4.5 h via flow cytometry. (E, F) BMDMs and peritoneal macrophages were treated with 100 ng/mL of LPS for 3 h and ROS was quantified using CM-H2DCFDA. (G) The mitochondrial ROS levels were monitored upon LPS treatment for 3 h using MitoSOX in BMDMs. (H) Mitochondrial membrane potential levels of BMDMs monitored upon LPS treatment for 3 h using MitoTracker™ Green FM and MitoTracker™ Red CMXRos. The data are presented as the ratio of red MFI/green MFI. (I) Raw264.7 cells were pre-treated with 20 nM FK866 or 0.5 mM NAD for 6 h and followed by LPS treatment for 6 h. These cells were subjected to measure ROS levels by using CM-H2DCFDA (left panel) and MitoSOX (right panel). The results are represented as the mean ± SEM. Statistical analysis was performed using the un-paired 2-tailed Student's *t*-test. . (For interpretation of the references to color in this figure legend, the reader is referred to the Web version of this article.)

NMN administration resulted in 67% survival (8/12 mice) (Fig. 7c). Next, we examined whether any cytotoxic side effects accompanied by NMN injection may present in mice. NMN administration did not alter body weights until 14 days (Supplementary Fig. 8b). No gross and microscopic abnormalities were observed in the colon, liver, or spleen at the same time point (Fig. 7d and Supplementary Fig. 8c). Furthermore, the serum levels of alanine aminotransferase (ALT) and aspartate aminotransferase (AST) were not increased upon NMN treatment (Fig. 7e), indicating that NMN injection could attenuate DSS-induced colitis without obvious hepatotoxicity. Consistently, NMN treatment increased Ki-67+ cells, while decreased cleaved caspase-3 and TUNEL signaling, with reduced F4/80$^{+}$ macrophage infiltration (Fig. 7f). These results that NMN administration protects mice from DSS-induced colitis by enhancing the resolution of inflammation.

## 4. Discussion

Herein, we demonstrated a fundamental role of NAMPT in macrophages using DSS-induced colitis model via the genetic ablation of *Nampt*. *Nampt* mKO mice suffered from prolonged, severe inflammation, although the initial inflammatory response was preserved regardless of NAMPT expression. NAMPT depletion did not affect the recruitment of macrophages or the production of inflammatory cytokines, whereas we found that NAMPT deletion impaired a "clean-up" process of macrophages, which is important in the resolution of inflammation and restoration of tissue homeostasis [3]. Deletion of NAMPT showed that clearance of tissue debris including apoptotic bodies was impeded due to reduced phagocytic activity, derived from insufficient NADPH supply. This functional deficit finally led to a prolonged, severe colitis in mouse model.

The data presented in this work provide several key insights into the role of macrophage-derived NAMPT within the inflammatory response, particularly in the context of IBD, which comprises CD and UC (chronic inflammatory disorders of the gastrointestinal tract). First, this is the first report that macrophage-specific NAMPT functions as a defensive measure to mitigates colitis severity with the genetic ablation of NAMPT in the myeloid compartment. Such findings do not agree with those of an earlier report that indicated that NAMPT inhibition, via a chemical

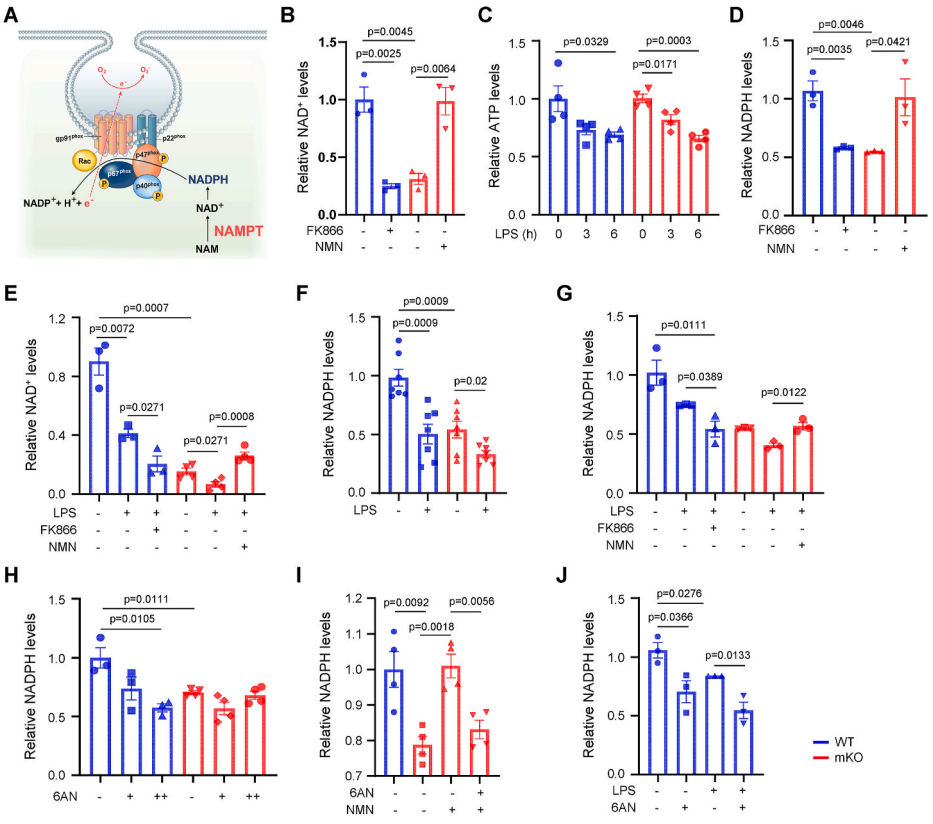


**Fig. 6.** NAMPT increases NADPH levels via PPP. (A) Schematic diagram. NAMPT enhances NOX2-mediated ROS generation via the increase of NADPH levels. (B) $NAD^+$ levels were measured after treatment with 20 nM FK866 or 2 mM NMN for 6 h in BMDMs from WT and *Nampt* mKO mice. (C) ATP levels were measured after treatment with 100 ng/mL LPS for 3 h or 6 h. (D) NADPH levels were measured treatment with 20 nM FK866 or 0.5 mM NMN for 6 h. (E–G) BMDMs were pretreated with 20 nM FK866 or 0.5 mM NMN for 6 h and then incubated with 100 ng/mL LPS for 6 h. $NAD^+$ levels (E) and NADPH levels (F, G). (H, I) NADPH levels were measured in present of 200 μM 6AN or 0.5 mM NMN. (J) BMDMs from WT mice were pretreated with 200 μM 6AN for 1 h. BMDMs were incubated with 100 ng/mL LPS for additional 3 h and subjected to NADPH measurement. Results shown are mean ± SEM. Statistical analyses were performed using an unpaired 2-tailed Student's *t*-test.

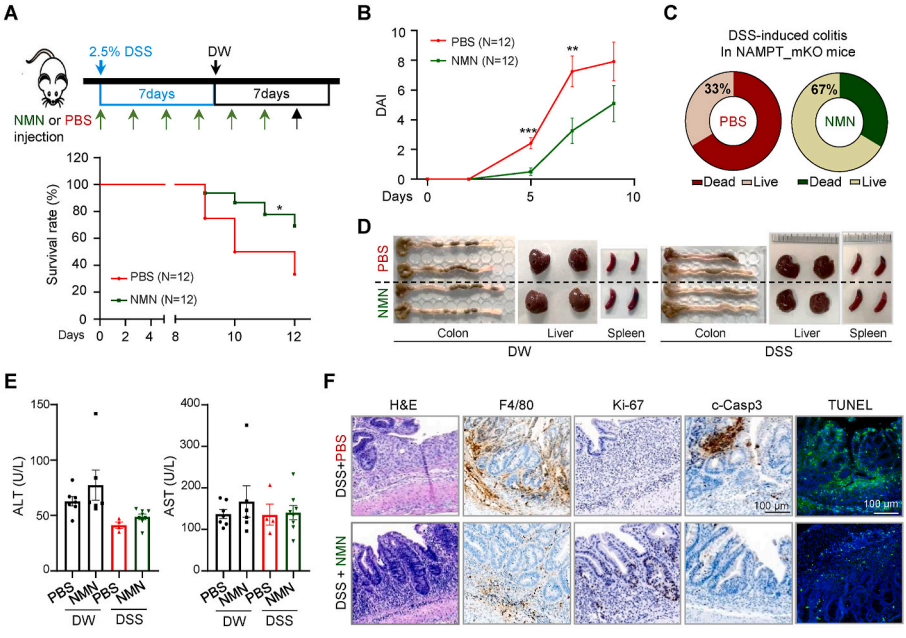


**Fig. 7.** NMN administration ameliorates the severity of DSS-induced colitis. *Nampt* mKO mice were treated with 2.5% DSS for 7 days and injected intraperitoneally with 500 mg/kg NMN or PBS at three times per week until termination of experiments. (A) Survival curve graph. (B) Disease activity index (DAI) was scored based on stool consistency, fecal bleeding, and weight loss as described in the materials and methods. (C) Venn diagram of survival rates. (D) Representative images of colon, liver, and spleen from DSS-treated *Nampt* mKO mice with or without NMN. (E) Serum ALT and AST levels (F) Immunohistochemical analysis from DSS-treated *Nampt* mKO mice upon NMN administration.

inhibitor, FK866, protects against inflammation in DSS-induced colitis [28]. This discrepancy probably due to a different model to demonstrate NAMPT function in inflammatory process. Since NAMPT expression is mainly in epithelial cells, enzymatic inhibition of NAMPT by FK866 could affect not only colon epithelial cells but also immune cells, thereby, inducing variable outcomes in inflammatory responses. Moreover, considering that chemical inhibitors might have exhibited off-target effects, FK866 may also elicit unknown effects aside from its impact on NAMPT enzymatic activity. Additionally, FK866 may affect function of circulating NAMPT, which is represented by secreted NAMPT from various cells, thereby, inducing distinct outcome in tissues [38,39]. Very recently, *Ratnayake* et al., reported that secreted NAMPT from the macrophage provides stem-cell-activating niche that promotes the muscle repair and regeneration by acting through C–C motif chemokine receptor type 5 (Ccr5) in mice [39]. In the line with this function of circulating NAMPT, inhibition of NAMPT by FK866 could cause loss of proliferation-inducing cues for injury-induced repair response in DSS-induced colitis. Although we did not determine whether

macrophage-secreted NAMPT promotes the colon repair and regeneration, comprehensive evidence from this study supports that macrophage-specific NAMPT functions to mitigate colitis severity.

Second, we found that NAMPT is essential in maintaining the phagocytic activity of macrophages. Inflammatory macrophages usually go through an oxidative burst, in which sufficient NADPH is required. Therefore, PPP: a metabolic pathway parallel to glycolysis, is highly activated to supply more NADPH in these cells [40]. Increased production of NADPH is used to generate ROS which is essential in the process of phagocytosis [36]. In this regard, transcriptional upregulation of NAMPT is also accompanied to meet the increased demand of NADPH in inflammatory macrophages, as depicted in Supplementary Figs. 4c–d. In fact, defect in the generation of NADPH, e.g., glucose-6-phosphate dehydrogenase (G6PD) deficiency, impairs ROS production and this results in severe and recurrent bacterial infections [10]. Therefore, our findings underscore the critical roles of the metabolic axis comprising NAMPT, NADPH, and ROS in the maintenance of phagocytic activity of macrophages.

Third, administration of NMN protects against deleterious inflammatory response in the DSS-induced colitis model of *Nampt* mKO mice without obvious toxic side effects. Despite this new therapeutic proposal, it might be misunderstood that the clinical translational relevance of our study seems to be limited, because the condition related to 'macrophage-specific NAMPT depletion' is not expected to be encountered easily in clinical setting. Eventually, we emphasize that $NAD^+$ is critical in the phagocytic activity of macrophages and in the subsequent resolution of inflammation. In cells, including macrophages, $NAD^+$ is largely made from nicotinamide (a form of vitamin B3, also known as niacin), which has various dietary sources, including fish, meat, and mushroom. Without proper supplementation, people can suffer from its deficiency, e.g., pellagra. Meanwhile, patients with IBD commonly suffer from poor oral intake because they frequently go through abdominal pain, diarrhea, or decreased appetite. Malabsorption is another common problem in IBD patients. Therefore, these challenges often result in nutritional imbalance or deficiency [41]. In fact, the reported prevalence of malnutrition in IBD patients ranges between 20% and 85% [42]. Furthermore, malnutrition is one of the most important factors associated with a poor clinical outcome in IBD patients [43,44]. Thus, this collective information implies that $NAD^+$ deficiency may occur in immune cells (which is equivalent to NAMPT depletion in macrophages in our study) of chronic IBD patients with malnutrition. In addition, ageing is accompanied by a gradual decline in tissue and cellular $NAD^+$ levels in multiple organisms including human [45,46]. This decline in $NAD^+$ levels is linked causally to numerous ageing-associated diseases, including cognitive decline, cancer, and metabolic disease [47–50]. Remarkably, it has been reported that NAMPT expression also decreases in many tissues during organismal aging [51–54]. Thus, it seems that decrease in $NAD^+$ is ascribed to the reduced NAMPT expression in aged cells, at least in part. Taken together, supplementation of NMN (or nicotinamide) seems to be an effective treatment strategy help to reduce the severity and the duration of inflammation in patients with IBD, in particular those who are old or suffer from malnutrition.

In summary, our data indicate that NAMPT in macrophages has a critical role in maintaining their phagocytic activity, which leads to proper resolution of inflammation and tissue repair. As $NAD^+$ might be deficient in IBD patients, supplementation of NMN appears to be an attractive therapeutic strategy. We hope that our approach activating the NAMPT-dependent $NAD^+$ biosynthetic pathway in order to control inflammatory diseases would provide new perspectives regulating inflammation and also open avenues for developing effective treatments.

## Author contributions

SM.H performed most of the experiments and analyzed the data. A-Y. L, SM.H, Y-J.H, M-J.K and S.M participated in the experiments. W.H, W–I.J, H–H.K, G.Y, and S–H.I provided technical support in the context of the *in vivo* model and intellectual support for data analysis. SM.K and HG.W analyzed publicly available data from IBD patients. D.L analyzed Immunohistochemistry data and clinical data from colitis patients provided technical support in the context of immunohistochemistry data performed pathological analyses. H-M.S, SM.H and D.L contributed to manuscript writing and discussion of the project. Y–S.K wrote the manuscript and supervised the study and takes responsibility for all of the data. All authors have read and approved the final manuscript.

## Funding

This work was supported by the National Research Foundation of Korea (NRF), funded by the Korea government [grant numbers 2021R1A4A1031856 and 2020R1C1C1007549]; and by a grant of the Korea Health Technology R&D Project through the Korea Health Industry Development Institute (KHIDI), funded by the Ministry of Health & Welfare, Republic of Korea [grant number HR21C1003].

## Declaration of competing interest

The authors have no competing interests to declare.

## Appendix A. Supplementary data

Supplementary data to this article can be found online at https://doi.org/10.1016/j.redox.2022.102237.

## References

[1] Y.R. Na, et al., Macrophages in intestinal inflammation and resolution: a potential therapeutic target in IBD, Nat. Rev. Gastroenterol. Hepatol. 16 (9) (2019) 531–543.
[2] G. Rogler, Resolution of inflammation in inflammatory bowel disease, Lancet Gastroenterol. Hepatol. 2 (7) (2017) 521–530.
[3] S. Watanabe, et al., The role of macrophages in the resolution of inflammation, J. Clin. Invest. 129 (7) (2019) 2619–2628.
[4] B. Luo, et al., Phagocyte respiratory burst activates macrophage erythropoietin signalling to promote acute inflammation resolution, Nat. Commun. 7 (2016) 12177.
[5] W. Yang, et al., Neutrophils promote the development of reparative macrophages mediated by ROS to orchestrate liver repair, Nat. Commun. 10 (1) (2019) 1076.
[6] A.M. Hine, P. Loke, Intestinal macrophages in resolving inflammation, J. Immunol. 203 (3) (2019) 593–599.
[7] S.J. Koo, N.J. Garg, Metabolic programming of macrophage functions and pathogens control, Redox Biol. 24 (2019) 101198.
[8] A.W. Roberts, et al., Tissue-resident macrophages are locally programmed for silent clearance of apoptotic cells, Immunity 47 (5) (2017) 913–927, e916.
[9] E.L. Falcone, et al., Colitis susceptibility in p47(phox-/-) mice is mediated by the microbiome, Microbiome 4 (2016) 13.
[10] W.C. Yen, et al., Impaired inflammasome activation and bacterial clearance in G6PD deficiency due to defective NOX/p38 MAPK/AP-1 redox signaling, Redox Biol. 28 (2020) 101363.
[11] L.A. Peters, et al., A functional genomics predictive network model identifies regulators of inflammatory bowel disease, Nat. Genet. 49 (10) (2017) 1437–1449.
[12] A. Rongvaux, et al., Pre-B-cell colony-enhancing factor, whose expression is up-regulated in activated lymphocytes, is a nicotinamide phosphoribosyltransferase, a cytosolic enzyme involved in NAD biosynthesis, Eur. J. Immunol. 32 (11) (2002) 3225–3234.
[13] A. Chiarugi, et al., The NAD metabolome–a key determinant of cancer cell biology, Nat. Rev. Cancer 12 (11) (2012) 741–752.
[14] G.S. Young, et al., Decreased cADPR and increased NAD+ in the Cd38-/- mouse, Biochem. Biophys. Res. Commun. 346 (1) (2006) 188–192.
[15] H.C. Ha, S.H. Snyder, Poly(ADP-ribose) polymerase is a mediator of necrotic cell death by ATP depletion, Proc. Natl. Acad. Sci. U. S. A. 96 (24) (1999) 13978–13982.
[16] J.R. Revollo, A.A. Grimm, S. Imai, The NAD biosynthesis pathway mediated by nicotinamide phosphoribosyltransferase regulates Sir2 activity in mammalian cells, J. Biol. Chem. 279 (49) (2004) 50754–50763.
[17] A. Garten, et al., Nampt: linking NAD biology, metabolism and cancer, Trends Endocrinol. Metabol. 20 (3) (2009) 130–138.
[18] A. Garten, et al., Physiological and pathophysiological roles of NAMPT and NAD metabolism, Nat. Rev. Endocrinol. 11 (9) (2015) 535–546.
[19] V. Audrito, V.G. Messana, S. Deaglio, NAMPT and NAPRT: two metabolic enzymes with key roles in inflammation, Front. Oncol. 10 (2020) 358.
[20] J.R. Revollo, et al., Nampt/PBEF/Visfatin regulates insulin secretion in beta cells as a systemic NAD biosynthetic enzyme, Cell Metabol. 6 (5) (2007) 363–375.

[21] S.H. Jia, et al., Pre-B cell colony-enhancing factor inhibits neutrophil apoptosis in experimental inflammation and clinical sepsis, J. Clin. Invest. 113 (9) (2004) 1318–1327.
[22] M.A. Nowell, et al., Regulation of pre-B cell colony-enhancing factor by STAT-3-dependent interleukin-6 trans-signaling: implications in the pathogenesis of rheumatoid arthritis, Arthritis Rheum. 54 (7) (2006) 2084–2095.
[23] M.E. Burczynski, et al., Molecular classification of Crohn's disease and ulcerative colitis patients using transcriptional profiles in peripheral blood mononuclear cells, J. Mol. Diagn. 8 (1) (2006) 51–61.
[24] D. Aran, Z. Hu, A.J. Butte, xCell: digitally portraying the tissue cellular heterogeneity landscape, Genome Biol. 18 (1) (2017) 220.
[25] X. Zhou, et al., YAP aggravates inflammatory bowel disease by regulating M1/M2 macrophage polarization and gut microbial homeostasis, Cell Rep. 27 (4) (2019) 1176–1189, e1175.
[26] D. Bauche, et al., LAG3(+) regulatory T cells restrain interleukin-23-producing CX3CR1(+) gut-resident macrophages during group 3 innate lymphoid cell-driven colitis, Immunity 49 (2) (2018) 342–352, e345.
[27] K. Moriwaki, et al., The necroptosis adaptor RIPK3 promotes injury-induced cytokine expression and tissue repair, Immunity 41 (4) (2014) 567–578.
[28] R.R. Gerner, et al., NAD metabolism fuels human and mouse intestinal inflammation, Gut 67 (10) (2018) 1813–1823.
[29] A. Ortega-Gomez, M. Perretti, O. Soehnlein, Resolution of inflammation: an integrated view, EMBO Mol. Med. 5 (5) (2013) 661–674.
[30] W. Zhu, et al., Disequilibrium of M1 and M2 macrophages correlates with the development of experimental inflammatory bowel diseases, Immunol. Invest. 43 (7) (2014) 638–652.
[31] R.A. Isidro, C.B. Appleyard, Colonic macrophage polarization in homeostasis, inflammation, and cancer, Am. J. Physiol. Gastrointest. Liver Physiol. 311 (1) (2016) G59–G73.
[32] T. Kawasaki, T. Kawai, Toll-like receptor signaling pathways, Front. Immunol. 5 (2014) 461.
[33] A.M. Cameron, et al., Inflammatory macrophage dependence on NAD(+) salvage is a consequence of reactive oxygen species-mediated DNA damage, Nat. Immunol. 20 (4) (2019) 420–432.
[34] I. Kourtzelis, G. Hajishengallis, T. Chavakis, Phagocytosis of apoptotic cells in resolution of inflammation, Front. Immunol. 11 (2020) 553.
[35] C.S. Lee, et al., Boosting apoptotic cell clearance by colonic epithelial cells attenuates inflammation in vivo, Immunity 44 (4) (2016) 807–820.
[36] O. Sareila, et al., NOX2 complex-derived ROS as immune regulators, Antioxidants Redox Signal. 15 (8) (2011) 2197–2208.
[37] S.M. Hong, et al., NAMPT suppresses glucose deprivation-induced oxidative stress by increasing NADPH levels in breast cancer, Oncogene 35 (27) (2016) 3544–3554.
[38] M.J. Yoon, et al., SIRT1-Mediated eNAMPT secretion from adipose tissue regulates hypothalamic NAD+ and function in mice, Cell Metabol. 21 (5) (2015) 706–717.
[39] D. Ratnayake, et al., Macrophages provide a transient muscle stem cell niche via NAMPT secretion, Nature (2021).
[40] A. Viola, et al., The metabolic signature of macrophage responses, Front. Immunol. 10 (2019) 1462.
[41] P. Balestrieri, et al., Nutritional aspects in inflammatory bowel diseases, Nutrients 12 (2) (2020).
[42] J. Goh, C.A. O'Morain, Review article: nutrition and adult inflammatory bowel disease, Aliment. Pharmacol. Ther. 17 (3) (2003) 307–320.
[43] I. Jansen, et al., Inflammation-driven malnutrition: a new screening tool predicts outcome in Crohn's disease, Br. J. Nutr. 116 (6) (2016) 1061–1067.
[44] A. Takaoka, et al., Nutritional screening and clinical outcome in hospitalized patients with crohn's disease, Ann. Nutr. Metab. 71 (3–4) (2017) 266–272.
[45] A.J. Covarrubias, et al., NAD(+) metabolism and its roles in cellular processes during ageing, Nat. Rev. Mol. Cell Biol. 22 (2) (2021) 119–141.
[46] J. Yoshino, J.A. Baur, S.I. Imai, NAD(+) intermediates: the biology and therapeutic potential of NMN and NR, Cell Metabol. 27 (3) (2018) 513–528.
[47] K.F. Mills, et al., Long-term administration of nicotinamide mononucleotide mitigates age-associated physiological decline in mice, Cell Metabol. 24 (6) (2016) 795–806.
[48] M. Yoshino, et al., Nicotinamide mononucleotide increases muscle insulin sensitivity in prediabetic women, Science 372 (6547) (2021) 1224–1229.
[49] J. Yoshino, et al., Nicotinamide mononucleotide, a key NAD(+) intermediate, treats the pathophysiology of diet- and age-induced diabetes in mice, Cell Metabol. 14 (4) (2011) 528–536.
[50] M. Yoshida, et al., Extracellular vesicle-contained eNAMPT delays aging and extends lifespan in mice, Cell Metabol. 30 (2) (2019) 329–342, e325.
[51] S. Johnson, D.F. Wozniak, S. Imai, CA1 Nampt knockdown recapitulates hippocampal cognitive phenotypes in old mice which nicotinamide mononucleotide improves, NPJ Aging Mech. Dis. 4 (2018) 10.
[52] E. Koltai, et al., Exercise alters SIRT1, SIRT6, NAD and NAMPT levels in skeletal muscle of aged rats, Mech. Ageing Dev. 131 (1) (2010) 21–28.
[53] R.N. Jadeja, et al., Loss of NAMPT in aging retinal pigment epithelium reduces NAD(+) availability and promotes cellular senescence, Aging (Albany NY) 10 (6) (2018) 1306–1323.
[54] H. Wang, et al., NAMPT reduction-induced NAD(+) insufficiency contributes to the compromised oocyte quality from obese mice, Aging Cell 20 (11) (2021), e13496.